Obour Institute Journal
for Engineering and Technology (OI-JET)
Journal homepage: https://oijet.journals.ekb.eg
Volume (1), Issue (1), December 2023

Fast and Stable Representation for Both Gray and Color 1-D or 2-DObjects Using Different Sets of Discrete Orthogonal Moments

Open access

Gaber Hassan: Department of Computer Science, Obour High Institute for Management & Informatics, Obour, Egypt, gaberh@oi.edu.eg
Mohamed S. Farag: Department of Computer Science, Obour High Institute for Management & Informatics, Obour, Egypt

Received August 10, 202٣, Revised September 5, 202٣, Accepted September 15, 202٣

Abstract

Representation, analysis and interpretation of an image acquired by a real (i.e. non ideal) imaging system is the key problem in many application areas such as robot vision, remote sensing, astronomy and medicine, to name but a few. Images may be gray or color. One of the most commonly used to represent gray images in the last period is the moments. Moments are considered as statistical quantities that describe the pixels distribution inside an image's space. Image reconstruction method is the best way to check the capability of the moment to represent the image efficiently. In this paper we introduced efficientmethods to reconstruct gray scale images based on various sets of discrete orthogonal moments: generalized laguerre moments (GLMs), Chebychev moments (CMs) and Krawtchouk moments (KMs). Assisted by quaternion algebra, representation of color images become smoothly, hence, we extended bothGLMs and CMs by using quaternion algebra and derived various sets of quaternion moments: quaternion generalized laguerre moments (Q_GLMs) and quaternion Chebychev moments (Q_CMs). The experimental results show the capacity of the proposed approaches for image reconstruction against different the noise attack. We used the normalized image reconstruction error (NIRE) as a measure to theimage reconstruction capability.

Keywords: *Discrete orthogonal moments; quaternion moments; image* reconstruction.

1. Introduction

In order to make decisions in our daily lives, each of us must virtually continually acquire, process, and analyze a vast amount of information of varying kinds, significance, and quality. More than 95% of the information we take in is visual. An image is an extremely potent information medium and communicationtool that can effectively and compactly portray complicated scenes and processes. As a result, images serve as important informational tools as well as tools for interpersonal communication and machine- human interaction. Common digital photos are incredibly information-rich. With a smartphone, you can snap a photograph and email it in a matter of seconds to your pals, packing as much information into onepicture as several hundred pages of prose. Automatic and potent picture analysis techniques are thus desperately needed.

It is possible to extract important information from digital photos by using the image descriptors knownas moments of orthogonal functions and transforms. Teague (M.R. Teague, 1980) defined orthogonal moments (OMs) as representing binary and grayscale images with the least amount of information overlap or redundancy. The OMs might be described in polar or Cartesian coordinates, with the polar OMs being known as circular orthogonal moments (P. George, 2014). While OMs of higher orders are able to extract the finer details of digitalimages, OMs of lower orders only extract global elements like forms, which is a very important procedure in distinguishing between identical images. Additionally, OMs exhibit decreased

Correspondence Author **Gaber Hassan** gaberh@oi.edu.eg

Print ISSN, 2974-4539, Online ISSN: 3062-5270

sensitivity to various types of noise. Analytically, the image intensity function might be reconstructed using a finite collection of OMs and the inverse moment transform. Because OMs are invariant to rotation, scaling, and translationtransformations, computer vision systems can distinguish between comparable images and objects regardless of orientation, location, and camera distance. The significant advantage of circular orthogonalmoments resides in their capacity to achieve rotation invariance due to their circular nature, which is a key attribute in pattern recognition applications (J. Flusser, T. Suk, B. Zitova, 2016). This is in addition to their ability to aid in picture reconstruction.

Moments are employed frequently in image processing and analysis because they may extract local and global identifying information from the image. In numerous applications, including image reconstruction [(B. Honarvar, et al 2014)(H. Karmouni, et al., 2017)(H. Zhu, et al. 2012)(M. Yamni, et al., 2019)(O. El ogri, et al., 2019)], image compression (B. Honarvar, et al 2014)(H. Rahmalan, et al., 2010) (G.A. Papakostas, et al., 2002)], image watermarking (E.D. Tsougenis, et al., 2015)(X. Liu, et al. 2017)(E.D. Tsougenis, et al., 2012) E.D. Tsougenis, et al., 2013)(L. Zhang, et al., 2007), edge detection (L.-M. Luo, et al., 1994), image geometric distortion correction (M. Alghoniemy, et al., 2000), and image classification [(A. Hmimid, et al., 2015) (M. Sayyouri, et al., 2015)], they are used with outstanding results. Projecting the data space on frequently orthogonal bases is the fundamental concept behind moments. In fact, discrete orthogonal polynomials [(A.F. Nikiforov, et al., 199)] like Chebichef , Krawtchouk, and Charlier and continuous orthogonal polynomials like Legendre,Zernike, Gegenbauer, and Fourier-Mellin form continuous orthogonal moments (COMs), and discrete orthogonal polynomials such as Chebichef [26], Krawtchouk, Charlier.

Laguerre moments Chebychev moments and Krawtchouk moments are three discrete orthogonal moments they are defined in terms of laguerre polynomial, Chebychev polynomial and Krawtchouk polynomial respectively. In this study we presented theses classical moments and their quaternion form for gray and color image representation via their ability to reconstruct such images.

2. Proposed discrete moments

2.1 Discrete Generalized Laguerre Moments (GLMs)

The ALMs are one kind of discrete orthogonal moment. It defined in the existence of the Laguerre polynomials (LPs) [33] (basis functions), which are orthogonal over the whole right-half plane. GLMs of the image $I(x, y)$ with the order of $m + n$ and size of $N\ x\ N$ are defined as follows:

$$\tilde{M}_{mn}^{\alpha}(x) = \sum_{x=0}^{N-1}\sum_{y=0}^{N-1} \tilde{L}_{m}^{\alpha}(x)\ \tilde{L}_{n}^{\alpha}(y)\ I(x,y), \qquad m,n = 0,1,2,\dots,N-1, \tag{1}$$

where, $\{L_m^{\alpha}\}$, for $\alpha > -1$ are the LPs that are orthogonal to the weight function $w(x) = x^{\alpha}e^{-x}$ on the interval $0 \le x \le +\infty$, that is

$$\int_0^{\infty} e^{-x}x^{\alpha}\, L_n^{\alpha}(x)\, L_m^{\alpha}(x)dx = \frac{\Gamma(n+\alpha+1)}{n!}\delta_{nm} \qquad m,n \ \ge 0, \tag{2}$$

where, δ_{nm} is a Kronecker delta, $\delta_{nm} = 1$ if $m = n$ and $\delta_{nm} = 0$ otherwise.
The LPs are defined as follows:

$$L_n^{\alpha}(x) = \sum_{k=0}^{n} \frac{(n+\alpha)!}{(n-k)!\,(k+\alpha)!\,k!}x^k, \tag{3}$$

The recurrence formula suitable for evaluation is

$$(n+1)L_{n+1}^{\alpha}(x) = (2n+1+\alpha-x)L_n^{\alpha}(x) - (n+\alpha)L_{n-1}^{\alpha}(x), \tag{4}$$

with the initial values

$$L_0^{\alpha}(x) = 1 \ and\ L_1^{\alpha}(x) = (\alpha+1-x), \tag{5}$$

but due to the high increase of the polynomial values with increasing of the order, we restrict our study with the normalized orthogonal LPs ($\tilde{L}_n^{\alpha}(x)$), that is defined as follows:

$$\tilde{L}_n^{\alpha}(x) = \sqrt{\frac{e^{-x}x^{\alpha}n!}{(n+k)!}}\, L_n^{\alpha}(x). \tag{6}$$

As shown in Fig. 1, one can observe that the values of the normalized polynomials $\tilde{L}_n^{\alpha}(x)$ are bounded on a finite interval, a thing that doesn't occur with non-normalized $L_n^{\alpha}(x)$. The value of the parameter α has an essential role in the pattern recognition task, where it controls the shifting to the image region ofinterest. In this study, we set the value of $\alpha = 2$.

2.2 Discrete Chebychev Moments (CMs)

The discrete Chebychev moments for digital image $I(x,y)$ defined as

$$\hat{\tau}_{mn} = \sum_{x=0}^{N-1}\sum_{y=0}^{N-1} \hat{T}_m(x)\ \hat{T}_n(y)\ I(x,y), \qquad m,n = 0,1,2,\dots,N-1, \tag{7}$$

where T_n refer to discrete Chebychev polynomials [34]. It defined in terms of the following recurrence formula

$$(n+1)T_{n+1}(x) = (2n+1)(2x-N+1)T_n(x) - n(N^2-n^2)T_{n-1}(x), n = 1,2,\dots \tag{8}$$

with the initial values

$$T_0(x) = 1 \ and\ T_1(x) = 2x+1-N. \tag{9}$$

But due to the high fluctuation that occurs with $T_n(x)$, as shown in Fig. 2, it would be more suitable to use the orthonormal polynomial $\hat{T}_n(x)$ whose norm equals one:

$$\sum_{x=0}^{N-1}\left(\hat{T}_n(x)\right)^2 = 1, \tag{10}$$

where $\hat{T}_n(x)$ defined in terms of the following recurrence formula

$$\hat{T}_n(x) = (\alpha_1 x + \alpha_2)\hat{T}_{n-1}(x) - \alpha_3\hat{T}_{n-2}(x), \tag{11}$$

with the initial values

$$\hat{T}_0(x) = \frac{1}{\sqrt{N}} \ and\ \hat{T}_1(x) = (2x+1-N)\sqrt{\frac{3}{N(N^2-1)}}, \tag{12}$$

where

$$\alpha_1 = \frac{2}{n}\sqrt{\frac{4n^2-1}{N^2-n^2}}, \tag{13}$$

$$\alpha_2 = \frac{1-N}{n}\sqrt{\frac{4n^2-1}{N^2-n^2}}, \tag{14}$$

$$\alpha_3 = \frac{n-1}{n}\sqrt{\frac{2n+1}{2n-3}}\sqrt{\frac{N^2-(n-1)^2}{N^2-n^2}}. \tag{15}$$

2.3 Discrete Krawtchouk Moments (KMs)

The Krawtchouk moments of order (n+m) in terms of weighted Krawtchouk polynomials, for an imagewith intensity function, $f(x,y)$, is defined as

$$\hat{K}_{mn} = \sum_{x=0}^{N-1}\sum_{y=0}^{N-1} \hat{K}_n(x;p,N)\,\hat{K}_m(y;p,N)\ f(x,y), m,n = ,0,1,2,\dots N-1 \tag{16}$$

The set of weighted Krawtchouk polynomials $\hat{K}_n(x;p,N)$ is defined by

$$\hat{K}_n(x;p,N) = K_n(x;p,N)\sqrt{\frac{w(x;p,N)}{\varrho(n;p,N)}}, \tag{17}$$

Where $K_n(x;p,N)$, $w(x;p,N)$ and $\varrho(n;p,N)$ are the classical Krawtchouk polynomials, weight function, and the normalization function, respectively, such that

$$K_n(x;p,N) = 2F1\left(-n,-x;-N;\frac{1}{p}\right) \tag{18}$$

$$w(x;p,N) = \binom{N}{x} p^x (1-p)^{N-x} \tag{19}$$

$$\varrho(n;p,N) = \left(\frac{1-p}{p}\right)^n \frac{1}{\binom{N}{n}}. \tag{20}$$

Classical Krawtchouk polynomials $K_n(x;p,N)$ an be defined as in the following recurrence formula

$$K_{n+1}(x;p,N) = \frac{Np-2np+n-x}{(N-n)p} K_n(x;p,N) - \frac{n(1-p)}{(N-n)p} K_{n-1}(x;p,N),$$
$$n = 1,2,\dots N-1 \tag{21}$$

where $K_0(x;p,N) = 1$ and $K_1(x;p,N) = 1 - \frac{x}{Np}$ are the initial values.

$K_n(x;p,N)$ satisfy the following orthogonality condition

$$\sum_{x=0}^{N} w(x;p,N) K_m(x;p,N) K_n(x;p,N) = \varrho(n;p,N)\delta_{mn}, \tag{22}$$

where, δ_{mn} is a kronecker delta, $\delta_{mn} = 1$ if $m = n$ and $\delta_{mn} = 0$ otherwise.

According to the above weight and normalization functions, the orthogonality condition of the weighted

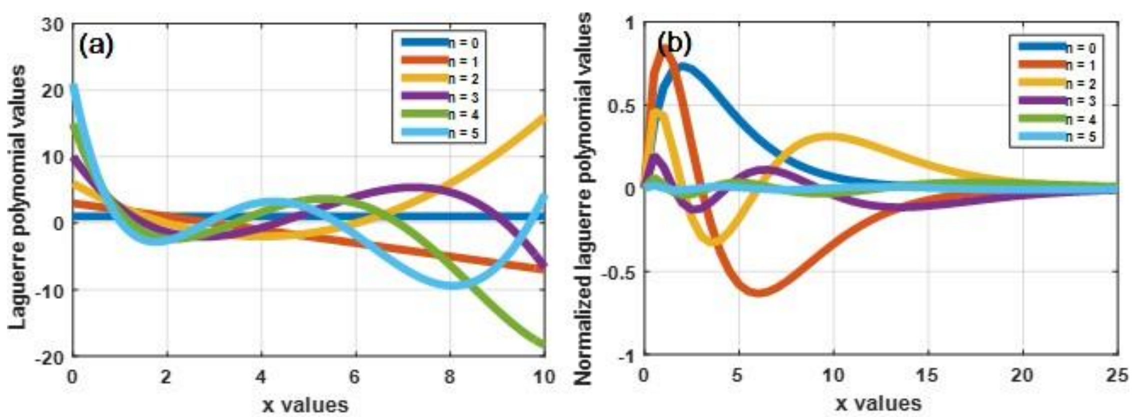

Fig. 1. Plot (a) $\mathbf{L}_n^{\alpha}(\mathbf{x})$, and (b) $\tilde{\mathbf{L}}_n^{\alpha}(\mathbf{x})$ at $\alpha = 2$.

Krawtchouk polynomials $\hat{K}_n(x;p,N)$ become as follows:

$$\sum_{x=0}^{N} \hat{K}_m(x;p,N)\hat{K}_n(x;p,N) = \delta_{mn}. \tag{23}$$

Fig. 3(a) shows the plots for the first few orders of the normalized Krawtchouk polynomials and

Fig. 3(a) shows the plots for the first few orders of the normalized Krawtchouk polynomials and

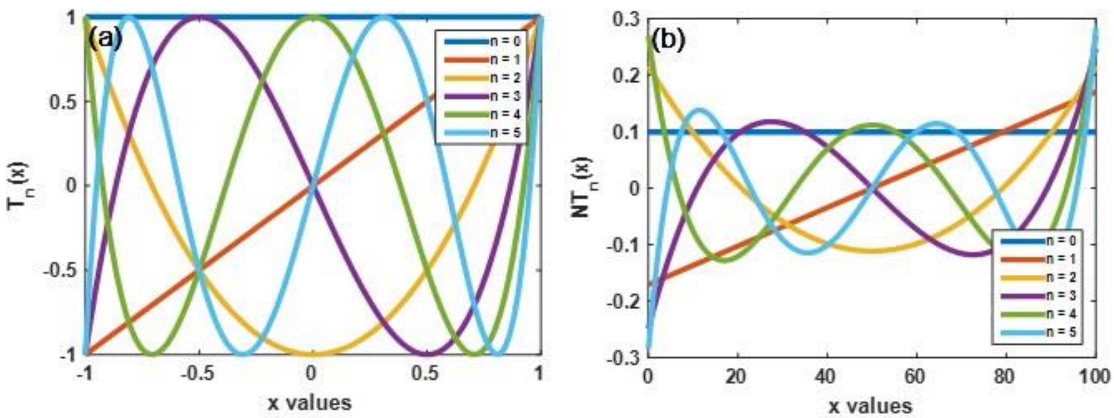

Fig. 2. Plot (a) $T_n(x)$, and (b) $\widehat{T}_n(x)$.

it is easily observed that the range of values of the polynomials expands rapidly with a slight increase of the order. The values of the weighted Krawtchouk polynomials are confined within the range of [-1, 1], as shown in Fig. 3(b).

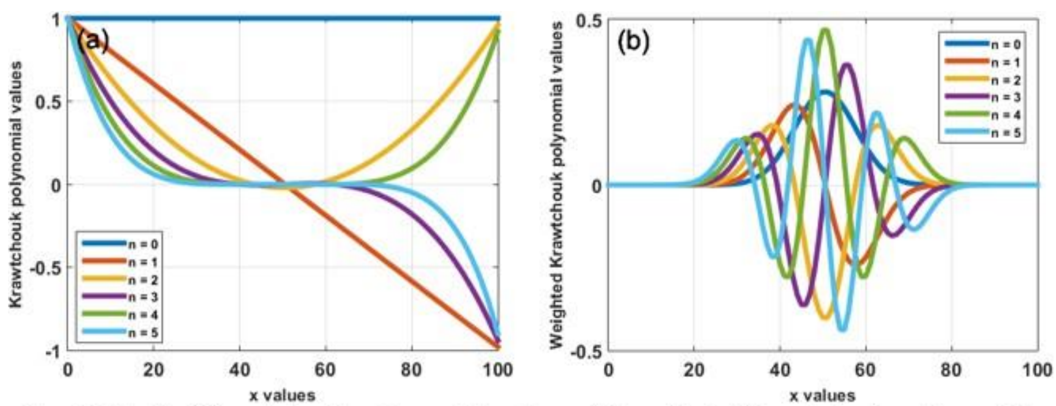

Fig. 3. Plot (a) Krawtchouk polynomial values, (b) weighted Krawtchouk polynomial values at $p = 0.5$.

2.4 Quaternion

In 1843 [46], Hamilton introduced a generalization to the complex number called quaternion. The complex number consists of two parts: the real part and another part called the imaginary part whereas, the quaternion consists of one real-part and the other three imaginary parts. The quaternion number q can be defined as follows:

$$q = a + bi + cj + dk, \tag{24}$$

where $a, b, c, d \in R$, and i, j, k represent complex operators have the following characteristics:

$$i^2 = j^2 = k^2 = -1, \tag{25}$$

$$ij = -ji = k, \quad jk = -kj = i, \quad ki = -ik = j. \tag{26}$$

Eq. (26) Shows that the multiplication in quaternions is not commutative.

Usually, it is better to represent the quaternion as a sum of two parts: a scalar part denoted as $S(q)$, and a vector part indicated as $V(q)$.

$$q = S(q) + V(q), \tag{27}$$

where $S(q) = a$ and $V(q) = bi + cj + dk$,

q is reduced to pure quaternion if $S(q) = 0$, and to unit pure quaternion if $\|q\| = 1$, where $\|q\| =$

$\sqrt{a^2+b^2+c^2+d^2}$.

2.5 Proposed Q_GLMs

Let $f(x, y)$ be an RGB color image defined in the cartesian coordinates. One can consider the three channels red, green and blue in the color image $f(x, y)$ as the three imaginary parts in pure quaternion, hence the color image $f(x, y)$ can be represented as follows:

$$f(x,y) = f_R i + f_G j + f_B k$$
$$= f_R(x,y)i + f_G(x,y)j + f_B(x,y)k. \quad (28)$$

Due to the noncommutative property of quaternion multiplication that appears in Eq. (26), there are two types of Q_GLMs: left-side Q_ALMs, and the right-side Q_GLMs.

In this study, we used the right-side Q_GLMs that can be defined as follows:

$$\tilde{Q}M_{mn}^{\alpha} = \sum_{x=0}^{N-1}\sum_{y=0}^{N-1} \tilde{L}_m^{\alpha}(x)\, \tilde{L}_n^{\alpha}(y)\, (if_R + jf_G + kf_B)\mu, \quad (29)$$

where μ is a pure unit quaternion chosen as $\mu = (i + j + k)/\sqrt{3}$ hence Eq. (29), rewritten as:

$$\tilde{Q}M_{mn}^{\alpha} = \frac{1}{\sqrt{3}}\sum_{x=0}^{N-1}\sum_{y=0}^{N-1} \tilde{L}_m^{\alpha}(x)\, \tilde{L}_n^{\alpha}(y)\, (if_R + jf_G + kf_B)(i + j + k)$$

$$\begin{aligned}
\tilde{Q}M_{mn}^{\alpha} = & -\frac{1}{\sqrt{3}}\sum_{x=0}^{N-1}\sum_{y=0}^{N-1} \tilde{L}_m^{\alpha}(x)\, \tilde{L}_n^{\alpha}(y)(f_R+f_G+f_B) \\
& + \frac{i}{\sqrt{3}}\sum_{x=0}^{N-1}\sum_{y=0}^{N-1} \tilde{L}_m^{\alpha}(x)\, \tilde{L}_n^{\alpha}(y)(f_G - f_B) \\
& + \frac{j}{\sqrt{3}}\sum_{x=0}^{N-1}\sum_{y=0}^{N-1} \tilde{L}_m^{\alpha}(x)\, \tilde{L}_n^{\alpha}(y)(f_B - f_R) \\
& + \frac{k}{\sqrt{3}}\sum_{x=0}^{N-1}\sum_{y=0}^{N-1} \tilde{L}_m^{\alpha}(x)\, \tilde{L}_n^{\alpha}(y)(f_R - f_G).
\end{aligned}$$

$$\tilde{Q}M_{mn}^{\alpha} = A_0^R + iA_1^R + jA_2^R + kA_3^R. \quad (30)$$

(R is a reference to right-side quaternion)

Where

$$\begin{aligned}
A_0^R = & -\frac{1}{\sqrt{3}}\sum_{x=0}^{N-1}\sum_{y=0}^{N-1} \tilde{L}_m^{\alpha}(x)\, \tilde{L}_n^{\alpha}(y)(f_R+f_G+f_B) \\
= & -\frac{1}{\sqrt{3}}[\sum_{x=0}^{N-1}\sum_{y=0}^{N-1} \tilde{L}_m^{\alpha}(x)\, \tilde{L}_n^{\alpha}(y)f_R
\end{aligned}$$

$$+\sum_{x=0}^{N-1}\sum_{y=0}^{N-1}\tilde{L}_m^{\alpha}(x)\,\tilde{L}_n^{\alpha}(y) f_G$$
$$+\sum_{x=0}^{N-1}\sum_{y=0}^{N-1}\tilde{L}_m^{\alpha}(x)\,\tilde{L}_n^{\alpha}(y) f_B],$$

$$A_0^R = -\frac{1}{\sqrt{3}}[\tilde{M}_{mn}^{\alpha}(f_R) + \tilde{M}_{mn}^{\alpha}(f_G) + \tilde{M}_{mn}^{\alpha}(f_B)]. \quad (31)$$

Similarly, as in Eq. (31)

$$A_1^R = \frac{1}{\sqrt{3}}[\tilde{M}_{mn}^{\alpha}(f_G) - \tilde{M}_{mn}^{\alpha}(f_B)]. \quad (32)$$

$$A_2^R = \frac{1}{\sqrt{3}}[\tilde{M}_{mn}^{\alpha}(f_B) - \tilde{M}_{mn}^{\alpha}(f_R)]. \quad (33)$$

$$A_3^R = \frac{1}{\sqrt{3}}[\tilde{M}_{mn}^{\alpha}(f_R) - \tilde{M}_{mn}^{\alpha}(f_G)]. \quad (34)$$

Thanks to the orthogonality property of Laguerre polynomial, the color images can be reconstructed easily from a finite number N of Q_GLMs using the following inverse moment transform:

$$\hat{f}(x,y) = \sum_{x=0}^{N-1}\sum_{y=0}^{N-1}\tilde{L}_m^{\alpha}(x)\tilde{L}_n^{\alpha}(y)\,\tilde{Q}M_{mn}^{\alpha}\,\mu,$$

$$+\frac{i}{\sqrt{3}}\sum_{x=0}^{N-1}\sum_{y=0}^{N-1}\tilde{L}_m^{\alpha}(x)\tilde{L}_n^{\alpha}(y)\,(A_0^R + A_2^R - A_3^R)$$

$$+\frac{j}{\sqrt{3}}\sum_{x=0}^{N-1}\sum_{y=0}^{N-1}\tilde{L}_m^{\alpha}(x)\tilde{L}_n^{\alpha}(y)\,(A_0^R - A_1^R + A_3^R)$$

$$+\frac{k}{\sqrt{3}}\sum_{x=0}^{N-1}\sum_{y=0}^{N-1}\tilde{L}_m^{\alpha}(x)\tilde{L}_n^{\alpha}(y)\,(A_0^R + A_1^R - A_2^R). \quad (35)$$

2.6 Proposed Q_CMs

Similarly, as in the case of right-side Q_ALMs, we deduced the right-side Q_CMs as:

$$\tilde{Q}CM_{mn}^{\alpha} = \sum_{x=0}^{N-1}\sum_{y=0}^{N-1}\hat{T}_m(x)\,\hat{T}_n(y)\,(if_R + jf_G + kf_B)\mu, \quad (36)$$

$$\tilde{Q}CM_{mn}^{\alpha} = \frac{1}{\sqrt{3}}\sum_{x=0}^{N-1}\sum_{y=0}^{N-1}\hat{T}_m(x)\,\hat{T}_n(y)\,(if_R + jf_G + kf_B)(i + j + k),$$

$$\tilde{Q}CM_{mn}^{\alpha} = A_0^R + iA_1^R + jA_2^R + kA_3^R. \quad (37)$$

Where

$$A_0^R = -\frac{1}{\sqrt{3}}[\hat{\tau}_{mn}(f_R) + \hat{\tau}_{mn}(f_G) + \hat{\tau}_{mn}(f_B)]. \quad (38)$$

$$A_1^R = \frac{1}{\sqrt{3}}[\hat{\tau}_{mn}(f_G) - \hat{\tau}_{mn}(f_B)]. \quad (39)$$

$$A_2^R = \frac{1}{\sqrt{3}}[\hat{\tau}_{mn}(f_B) - \hat{\tau}_{mn}(f_R)]. \quad (40)$$

$$A_3^R = \frac{1}{\sqrt{3}}[\hat{\tau}_{mn}(f_R) - \hat{\tau}_{mn}(f_G)]. \quad (41)$$

The reconstructed color image can be obtained similarly, as in Equ. 35.

3. Results and Discussion

3.1 Experimental results over gray scale and color images

This section presents the test data and results used to validate the theoretical framework presented above, and also to establish the feature representation capability of Generalized Laguerre moments (GLMs) Chebychev moments (CMs) and Krawtchouk moments (KMs) through image reconstruction. A

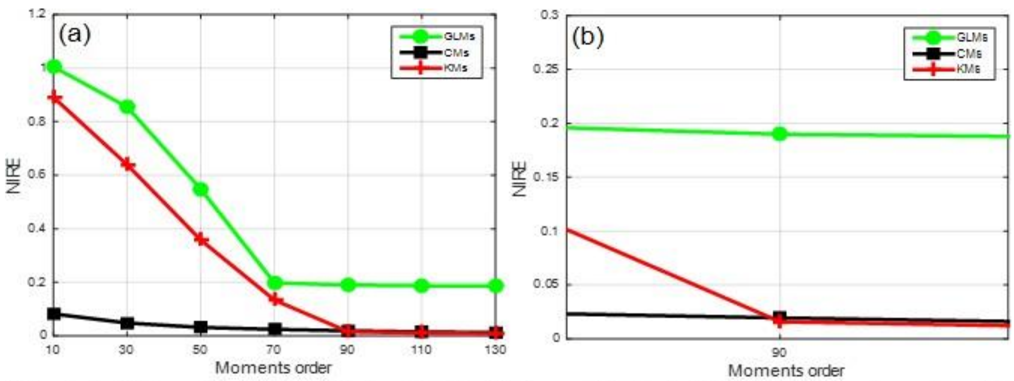

Fig. 4. (a) The values of NIRE for GLMs, CMs and KMs at different moments order, (b) zoom for more clarification.

comparative analysis between the proposed approaches is also given. An objective measure is used to characterize the error between the original image, $f(x, y)$, and the reconstructed image, $f(x, y)$, is defined as follows:

$$NIRE = \frac{\sum_{x=0}^{N-1}\sum_{y=0}^{N-1}\left(f(x,y) - \hat{f}(x,y)\right)^2}{\sum_{x=0}^{N-1}\sum_{y=0}^{N-1}\left(f(x,y)\right)^2}, \qquad (42)$$

A gray scale image of Cameraman (see Fig. 5) on a 256 x 256 pixel grid was used to analyze the values of the moment functions. As shown in Figs. 4 and 5 the obtained NIRE values and the reconstructed images specified that the Chebychev moments give better results at low orders but at orders greater than 90, Krawtchouk moments were the best. The same results obtained with the true colors as specified in Figs (6) and (7).

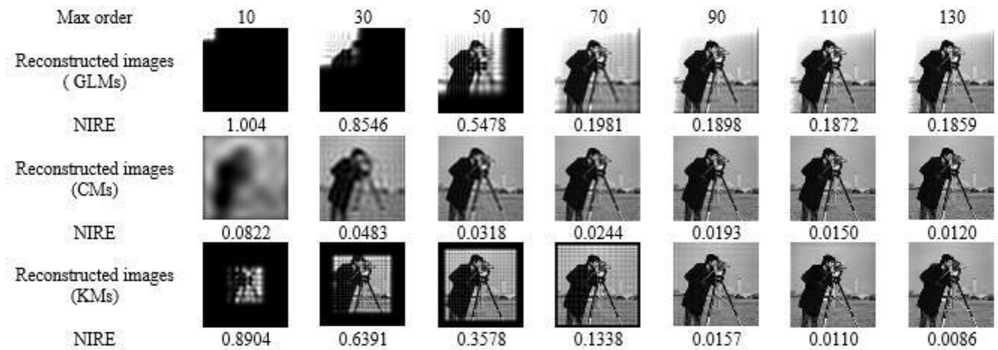

Fig. 5. The reconstructed gray scale image Cameraman using the proposed methods.

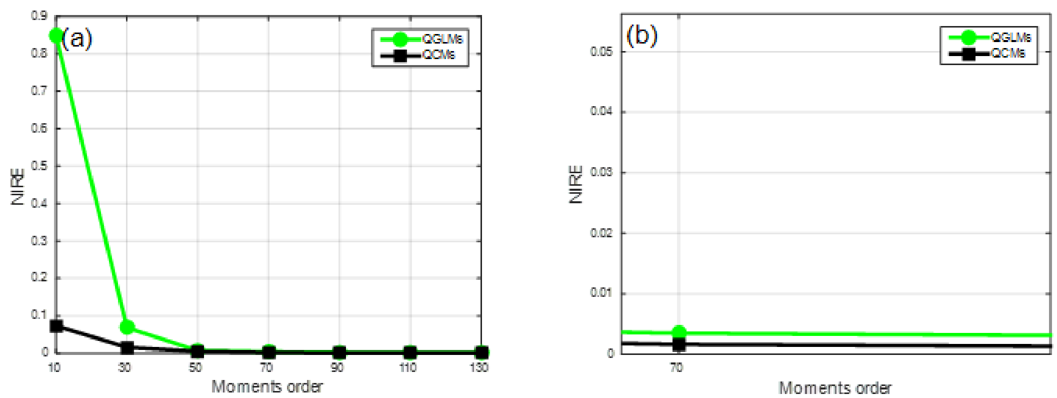

Fig. 6. The values of NIRE for Q_GLMs and Q_CMs at different moments order.

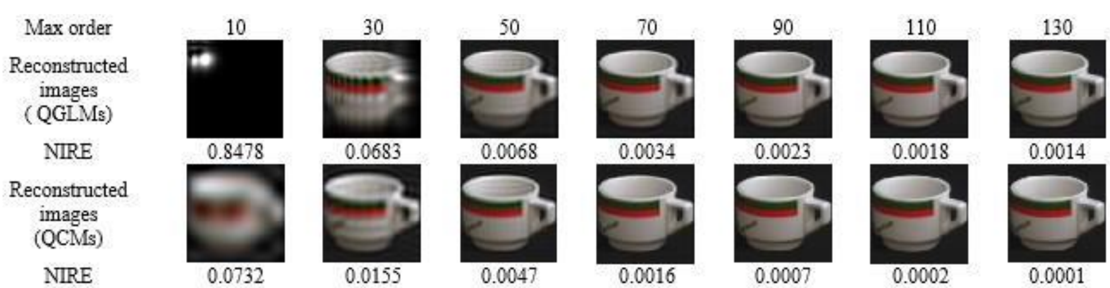

Fig. 7. The reconstructed color image using the proposed methods: Q_GLMs and Q_CMs.

4. Conclusion

In this study, three sets of discrete Generalized Linear Model moments are The polynomials Laguerre, Chebyshev, and Krawtchouk are introduced. The polynomials are scaled before the suggested moments are formulated, creating a new set of weighted polynomials. By doing so, overflows are prevented and the polynomials' dynamic range of values is constrained. There is no requirement for spatial quantization because the weighted polynomials are polynomials of a discrete variable, hence the proposed moments can be calculated without the use of numerical approximation. This characteristic makes the suggested moments ideal for obtaining the analytical characteristics of digital images. We also introduced sets of quaternion Generalized Laguerre and quaternion Chebyshev moments for representation of true color images. The reconstructed images test specified the superiority of the Krawtchouk moments at higher orders in both cases of gray scale and color images.

References

5. -A. Hmimid, et al., Fast computation of separable two-dimensional discrete invariant moments for image classification, Pattern Recognit. 48 (2) (2015) 509–521.

6. -A. Khotanzad, et al., Invariant image recognition by Zernike moments, IEEE Trans. Pattern Anal. Mach. Intell. 12 ((5)May) (1990) 489–497, doi:10.1109/ 34.55109.

7. -A. Mesbah, et al., Fast algorithm for 3D local feature extraction using Hahn and Charlier moments, in: International Symposium on Ubiquitous Networking, 2016, pp. 357–373.

8. -A.F. Nikiforov, et al., Classical orthogonal polynomials of a discrete variable, in: Classical Orthogonal Polynomials of a Discrete Variable, Springer, 1991, pp. 18–54.

9. -B. Honarvar, et al., Fast computation of Krawtchouk moments, Inf. Sci. 288 (December) (2014) 73–86,doi:10.1016/j.ins.2014.07.046.

10. -B. Honarvar, et al., Image reconstruction from a complete set of geometric and complex moments, Signal Process. 98 (May)(2014) 224–232, doi:10.1016/ j.sigpro.2013.11.037.

11. -B.H.S. Asli, et al., New discrete orthogonal moments for signal analysis, Signal Process 141 (2017) 57–73.

12. -C.-W. Chong, et al., Translation and scale invariants of Legendre moments, Pattern Recognit. 37 ((1) January) (2004)119–129, doi:10.1016/j.patcog.2003.06. 003.

13. Conference on Advanced Technologies for Signal and Image Processing (ATSIP), 2017, pp. 1–5.

14. -E.D. Tsougenis, et al., Image watermarking via separable moments, Multimed. Tools Appl. 74 (11) (2015) 3985–4012.

15. -E.D. Tsougenis, et al., Introducing the separable moments for image watermarking in a tottaly moment-oriented framework, in: 2013 18th International Conference on Digital Signal Processing (DSP), Fira , Santorini , Greece, 2013,pp. 1–6, doi:10.1109/ICDSP.2013.6622813.

16. -E.D. Tsougenis, et al., Performance evaluation of moment-based watermarking methods: a review, J. Syst. Softw. 85 (8) (2012) 1864–1884.

17. -Faculty of Technical Mathematics and Informatics, Tech. Univ. Delft, The Netherlands, Tech. Rep. 98-17,", 1998.

18. -G. Szego, Orthogonal Polynomials, 4th ed. New York: Amer. Math. Soc., 1975, vol. 23.

19. -G.A. Papakostas, et al., Image coding using a wavelet based Zernike moments compression technique, in: 2002 14th International Conference on Digital Signal Processing Proceedings. DSP 2002 (Cat. No. 02TH8628), 2, 2002, pp. 517–520.

20. -H. Karmouni, et al., Fast and stable computation of the Charlier moments and their inverses using digital filters and imageblock representation, Circuits Syst. Signal Process. 37 ((9) September) (2018) 4015–4033, doi:10.1007/ s00034-018- 0755-2.

21. -H. Karmouni, et al., Image analysis using separable Krawtchouk–Tchebichef's moments, in: 2017 International

22. -H. Karmouni, et al., Image reconstruction by Krawtchouk moments via digital filter, in: 2017 Intelligent Systems andComputer Vision (ISCV), 2017, pp. 1–7.

23. -H. Rahmalan, et al., Using tchebichef moment for fast and efficient image compression, Pattern Recognit. Image Anal. 20(4) (2010) 505–512.

24. -H. Zhu, et al., General form for obtaining discrete orthogonal moments, IET Image Process 4 (5) (2010) 335, doi:10.1049/iet- ipr.2009.0195.

25. -H. Zhu, et al., Image representation using separable two-dimensional continuous and discrete orthogonal moments, PatternRecognit. 45 (4) (2012) 1540–1558.

26. -J. Flusser, T. Suk, B. Zitova, 2D and 3D Image Analysis By Moments, John Wiley & Sons, 2016 ISBN: 9781119039372.

27. -K.M. Hosny, Image representation using accurate orthogonal Gegenbauer moments, Pattern Recognit. Lett. 32 ((6) April)(2011) 795–804, doi:10.1016/j. patrec.2011.01.006.

28. -L. Zhang, et al., Geometric invariant blind image watermarking by invariant tchebichef moments, Opt. Express 15 (5) (2007) 2251, doi:10.1364/OE.15. 002251.

29. -L.-M. Luo, et al., A modified moment-based edge operator for rectangular pixel image, IEEE Trans. Circuits Syst. VideoTechnol. 4 (6) (1994) 552–554.

30. -M. Alghoniemy, et al., Geometric distortion correction through image normalization, in: 2000 IEEE International Conference on Multimedia and Expo. ICME2000. Proceedings. Latest Advances in the Fast Changing World of Multimedia (Cat. No. 00TH8532), 3, 2000, pp. 1291–1294.

31. -M. Sayyouri, et al., Image classification using separable invariant moments of Krawtchouk-Tchebichef, Int. Conf. Comput.Syst. Appl. (2015) 1–6.

32. -M. Yamni, et al., Influence of Krawtchouk and Charlier moment's parameters on image reconstruction and classification,

33. -M.R. Teague, Image analysis via the general theory of moments, J. Opt. Soc. Am. 70 (8) (1980) 920–930.

34. -O. El ogri, et al., 2D and 3D Medical Image Analysis by Discrete Orthogonal Moments, Procedia Comput. Sci. 148 (2019)428–437.

35. -P. George , Over 50 years of image moments and moment invariants, Moments and Moment Invariants – Theory andApplications, Science Gate Publishing, 2014, pp. 3–32. ISBN 978-618-81418-0-3.

36. Procedia Comput. Sci. 148 (2019) 418–427.

37. -R. Mukundan, et al., Image analysis by Tchebichef moments, IEEE Trans. Image Process. 10 (9) (2001) 1357–1364.

38. -R. W. Askey, J., Associated Laguerre, and Hermite Polynomials, *Proc. Roy. Soc. Edinburgh Sect*, **96**:15, 1984.

39. -T. Jahid, et al., Image moments and reconstruction by Krawtchouk via Clenshaw's reccurence formula, Int. Conf. ElectricalInf. Technol. (2017) 1–7.

40. -X. Liu, et al., Fractional Krawtchouk transform with an application to image watermarking, IEEE Trans. Signal Process.65 ((7) April) (2017) 1894–1908, doi:10.1109/TSP.2017.2652383.

41. -Y. Sheng, et al., Orthogonal Fourier–Mellin moments for invariant pattern recognition, JOSA A 11 ((6) June) (1994)1748–1757, doi:10.1364/JOSAA.11. 001748